

Quantized thermal conductance in metallic heterojunctions

T. Lakshmi,

Assistant Professor, Department of Humanities and Science, Samskruti College of Engineering and Technology, Ghatkesar

ABSTRACT

It is critical to understand how charge and heat are transferred at the nanoscale in order to create next-generation electronics and high-efficiency energy-harvesting devices for future applications. When it comes to probing the quantum limitations of transport, metallic atomic-size contacts are perfect systems. Several recent studies have shown that the thermal conductance and electrical conductance of gold atomic contacts may be quantized at room temperature. However, the quick breaking dynamics of metallic junctions at room temperature, which might surpass the average reaction time of the thermal measurement, represents a significant experimental barrier in such studies. An integrated heater that also serves as a thermometer is used in this break-junction arrangement, which combines Scanning Tunneling Microscopy with suspended microelectromechanical systems with a gold-covered membrane. Other metals, including as Pt, PtIr, and W, were used as tip materials instead of gold to demonstrate heat transfer measurements across single gold atomic contacts. The relationship between thermal conductivity and contact size is investigated as a function of the contact size and the materials employed. In our experiments, we have discovered that by utilising Pt and Pt-Ir tips, we may increase the mechanical stability and likelihood of creating single Au atomic connections. In the next section, we demonstrate the quantization of electrical and thermal conductances, followed by a demonstration of the Wiedemann-Franz law at the atomic scale. We anticipate that these discoveries will expand the flexibility of experimental methodologies for examining heat transport in metallic quantum point contacts, as well as the ability to investigate the thermal characteristics of molecular junctions.

Introduction:

The investigation of the heat transport characteristics of nanoscale metallic contacts is of critical importance for the scaling of electrical interconnects because of their small size and low resistance. Metallic atomic-scale contacts represent the absolute size limit and have been employed as ideal systems to test electrical conductance quantization over the last several decades¹. Meanwhile, they were used as electrodes to make contact with single organic molecules and investigate the charge transport capabilities of such molecules.²

It is possible to see quantization effects when the size of the conductor

is equivalent to the wavelength of the charge carriers (F). Due to the fact that the typical transversal size of about a few atoms is on the order of the Fermi wavelength of the metal ($F = 0.5 \text{ nm}$) and the length (up to few nm in the case of atomic chains) are both well below the electron mean free path (10–100 nm) at room temperature, metallic atomic contacts are classified as quantum one-dimensional ballistic systems in this context.^{1,3} Charge transport in this regime is often characterised using the Landauer-Büttiker formalism⁴, which connects the electrical characteristics of the mesoscopic

conductor with the quantum mechanical transmission and reflection probabilities of the electron wavefunctions.⁴

Break-Junction methods, such as Scanning Tunneling Microscopy with Break Junctions (STM-BJ) or Mechanically Controlled Break Junctions (MCBJ), have been used extensively to investigate the quantization of electrical conductance in atomic junctions (MCBJ).

2 In these approaches, the electrical conductance is measured by repeatedly creating and breaking nanoscopic metallic contacts while the electrical conductance is measured. As a result of the quantization effects and atomic rearrangements, the breaking process is characterised by a gradual reduction in electrical conductance. 5 The production of single atom connections prior to total rupture is characterised by the establishment of a distinctive conductance value that is dependent on the number of electronic channels accessible for conduction and the likelihood of transmission of those channels. 6 Example: Single gold-atom contacts have an electrical conductance of 1 G_0 , where the electrical conductance quantum $G_0 = 2e^2/h$ is defined as the electron charge divided by the Planck constant. This corresponds to a single electron channel with complete transmission and spin degeneracy.

As a result, the break junction technique has been extended to explore heat dissipation in such atomic junctions as well as thermoelectric effects in such atomic junctions as well as thermal transport^{11,12}. A direct relationship between heat dissipation and thermoelectric qualities has been established, and this relationship has been proven in terms of the energy dependency of the transmission

function. ^{7,13} Furthermore, heat transport in gold and platinum atomic contacts is dominated by electrons with low phonon contribution¹⁴, which is consistent with the Wiedemann-Franz law^{11,15}, which stipulates that electrons dominate heat transport in atomic contacts.

$$G_{th} = L_0 T G_{el},$$

The heat transfer through gold atomic contacts was investigated in a recent experiment¹¹ in which we used electrochemically etched gold tips on suspended MicroElectro-Mechanical Systems (MEMS) with integrated microheaters in a custom-built scanning tunnelling microscope (STM). In this paper, we look at the possibility of how the material of the tip affects the heat transport qualities of the material. Atomic interactions made of gold. Interestingly, we discover that electrochemically Pt and Pt-Ir etched tips may be utilised without additional treatment to create a variety of shapes. MEMS sensors with better performance are formed by forming Au atomic connections. Mechanical stability is shown by a thermal conductivity that is in excellent accord with the Wiedemann-Franz equation. Pt-Ir alloys and tungsten carbide are the tip materials of choice for STM imaging. Because of their longevity, mechanical stability, and simplicity of manufacture, W are preferred. Indeed, early STM-BJ investigations were carried out using electrochemical etching.^{16,17} the W or Pt-Ir point into a softer metal surface such as Au was used to get the desired result. The surface of the tip is covered after a few indentation stages. In comparison to studies with pure Au, no change is detected in the electrical conductance traces and histograms when Au atoms are used in the experiments. tips.^{18–20} This phenomena may be explained by adhesion generated by the

environment. the wetting of the hard tip by the softer metal, resulting in the formation of an atomically thin layer above the apex of the tip. However, in order to prevent errors in the chemical composition of the metallic contact created, the same substance was used for both the test and the control. In break junctions, the tip and the surface have traditionally been chosen based on their characteristics. In particular, while studying electrical engineering, this is critical. The characteristics of organic molecules are influenced by the binding configuration and the electrode work function to a significant degree. Heat transport measures impose new restrictions on the top of the iceberg. The effects of radius and atomic junction stability on STM-BJ measurements are normally not a source of concern because of their small magnitudes. Using a manual cutter, cut tips for example, because of their high apex radius and irregular shape, which increases the likelihood of parasitic contact developing, they are not ideal for this application. Adsorbates on the surface of the liquid as a result, nanometer-sized tips are used, which may be produced quickly and readily by electrochemical etching of metal wires. Gold tips that have been electrochemically etched, on the other hand, are often used. Mechanically fragile, and it has the potential to cause undesirable plastic deformity, reducing the yield in the break junction measurement during the break junction measurement results. Another significant factor to consider when measuring heat transfer is the contact's atomic lifetime is measured in seconds. This is done by the measurement of thermal conductivity. The heat capacitance has

an inherent time constant that is proportional to the time constant as well as the heat resistance of the MEMS sensor, which is in the range of a few tens of milliseconds. This specifies the shortest amount of time necessary to measure. In contrast to electrical conductance, the thermal conductance of a single atom is measured. In this scenario, the measurement bandwidth is solely restricted by the external measurement bandwidth. For the purpose of determining the impact of various tip materials on the heat transport measurements, we produced Au, Pt, Pt-Ir (80–20 percent) and W in order to conduct transport measurements by electrochemical etching using established recipes and by electrochemical etching. Obtaining tip sizes of less than 100 nm. a comprehensive description of the supplemental material contains information on the manufacturing process for the various metals available. After that, the thermal conductance measurements were performed using MEMS sensors in the same manner as previously stated. In a nutshell, Figure 1 shows a MEMS device made up of a suspended silicon nitride membrane with an embedded platinum microheater that is in thermal equilibrium with a gold platform that is used to create and break contacts with the tip (a). It is intended to be used. Should have a high thermal resistance (2.5 10⁷ K/W) and an expected electrical resistance. The lateral rigidity is around 100 N/m.

The samples are cleaned with acetone before being used in the measurement. The use of oxygen plasma (400W for 5 minutes) to eliminate organic residues is then recommended. put into the vacuum chamber and allowed to build up until

the internal pressure was reached achieves a pressure of 107 mbar. Throughout the experiment, the tip and the sample were used. Because of this, the substrate is thermally tethered to ambient temperature (22 C).to the mechanical connections that connect the remainder of the setup

The STM was created just for you. The equipment is placed in the IBM Noise Free Labs, which ensures that the temperature is controlled. The laboratory environment has a temperature stability of 0.01 C. 27 The STM tips were tested first by performing electrical STM-BJ measurements at a set modest voltage below 50 mV on a non-suspended electrode. Gold pad patterning on the substrate, which has also been subjected to the same treatment

The gold platform on the MEMS is created during the manufacturing and cleaning stages. It should be noted that the electrical current is measured using a series resistance of As a result, the actual voltage drop across the junction is determined by 13 kX. based on the resistance of the connection itself

The findings are summarised in the following section: Fig. 1: A diagram of the measurement setup showing the MEMS sensor in contact with the STM tip. (b) SEM micrograph of the MEMS sensor. (c) Electrical conductance histograms obtained with different tip materials on a non-suspended gold pad, built from 1000 opening traces using linear binning with a bin size of 0.025 G0. (d) Electrical histograms with tips made out of Pt, Pt-Ir, and Au on the MEMS, built with, respectively, 1700, 2000, and 2000 traces using linear binning with a bin size of 0.025 G0

Fig. 2: (a)–(c) 2D and 1D histograms of thermal versus electrical conductance for atomic Au contacts measured with Au, Pt, and Pt-Ir tips, built with, respectively, 738, 877, and 982 traces, showing plateaus between 0.8 and 1.3 G0 which are at least 10 ms in duration. (d)–(f) Examples of single opening traces measured with different tip

the chemical species present at the junction that are involved in the process

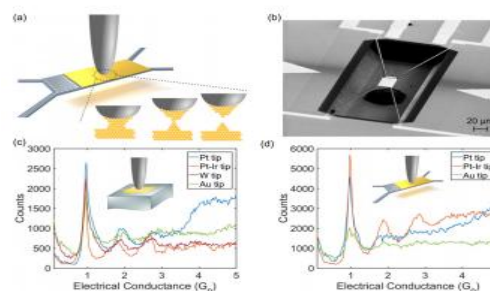


FIG. 1. (a) Schematic of the measurement setup showing the MEMS sensor in contact with the STM tip. (b) SEM micrograph of the MEMS sensor. (c) Electrical conductance histograms obtained with different tip materials on a non-suspended gold pad, built from 1000 opening traces using linear binning with a bin size of 0.025 G0. (d) Electrical histograms with tips made out of Pt, Pt-Ir, and Au on the MEMS, built with, respectively, 1700, 2000, and 2000 traces using linear binning with a bin size of 0.025 G0

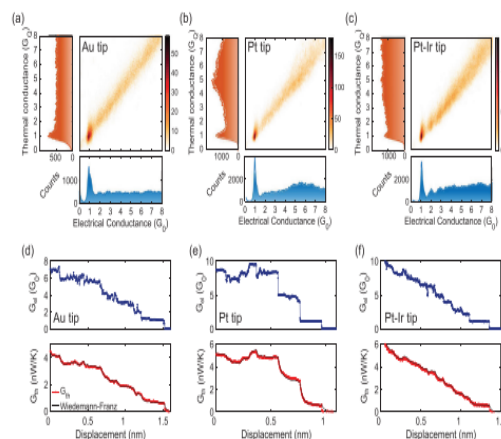


FIG. 2. (a)–(c) 2D and 1D histograms of thermal versus electrical conductance for atomic Au contacts measured with Au, Pt, and Pt-Ir tips, built with, respectively, 738, 877, and 982 traces, showing plateaus between 0.8 and 1.3 G0 which are at least 10 ms in duration. (d)–(f) Examples of single opening traces measured with different tip

materials. The black continuous line in the thermal conductance plot is calculated by applying the Wiedemann-Franz law to the digitally low-pass filtered electrical trace

Due to the fact that d-wave metals such as Pt and Ir, which have also been shown to create single atom connections, do not exhibit conductance quantization, the single atom conductance for these metals is between 1.5 and 2 G₀. 28–30 When using PtAu and Pd-Au metal alloys, the single atom peak at 1 G₀ was seen in the conductance histograms up to a gold content of less than 50%. 31,32 Figure 1(d) shows the results produced by using comparable tips on the same surface. MEMS, which was heated to around 60 degrees Celsius in order to test the thermal conductivity. The junction's transport features are described below. W was used to obtain 11 measurements. Tips on the MEMS provide ambiguous results, which is most likely due to the fact that in conjunction with the MEMS mechanics, a rapid oxidation of the tip surface is achieved. With Pt and Pt-Ir tips, on the other hand, we found considerable oxidation. The creation of a single gold atomic nucleus is shown by the peak at 1 G₀ contacts. If the tips were utilised first, the histograms were quite similar to what was produced. The presence of a gold substrate or direct contact with the MEMS indicates that the decreased stiffness of the MEMS sensors had no effect on the wetting of the Au. process.

On average, we can see that the electrical conductance histograms recorded with Pt and Pt-Ir tips have a higher number of peaks than those observed with other tips. 1 G₀ is the starting point for counting. This might be the outcome of an increased likelihood of creating a bond. Single

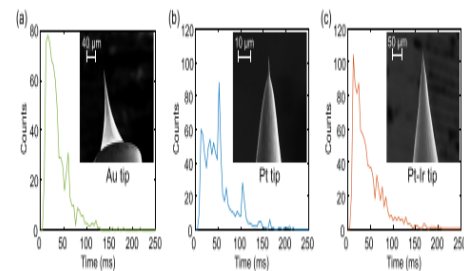
Au atom connections or an improvement in junction stability are also possible outcomes. All of the datasets were collected at a constant voltage of 40 millivolts (mV), having a sampling rate of one millisecond and a pulling speed ranging between two and four nanometers per seconds in the direction of the motion of the tip

Indeed, the tip is always present on the gold pad that is not hanging. When the tip of the MEMS is approached perpendicular to the surface, it is generally moved at lesser angles to take advantage of the greater in-plane surface area. rigidity and increase mechanical control over the breaking process, so preventing big jumps out of contacts, are two objectives. 11 In order to conduct these studies, The angles of approach were varied between 20 and 30 degrees, with no discernible effects. The electrical and thermal resistances were then measured concurrently. The conductivity of Au-Au interactions with various tips is measured. During the course of the In this experiment, the MEMS is heated to a temperature of TH 60 C by the researcher. the Pt-heater is subjected to a constant voltage that corresponds to just a few IW power that has been squandered. The temperature of the membrane is continually monitored by measuring the resistance of the Pt-4-probe heater's probes on a continuous basis. utilising the temperature coefficient of resistance that was previously calibrated, and

$$R(T) = R_0(1 + \alpha\Delta T),$$

where R₀ represents the resistance of the heater 4P at room temperature. In order to compute the overall thermal conductance of the tip-MEMS system, divide the total power wasted in the heater by the temperature difference between the two

temperatures. D T 14 T_H T_{amb} is the distance between the membrane and the tip/substrate. After that, the thermal conductance of the Au-Au contacts is calculated by deducting the value for being out of contact (tip in the tunnelling regime), in which the MEMS contributes, and the incontact one, which comprises both the MEMS and non-contact contributions, respectively. The Au-Au intersection. Examples of thermal and electrical conductance opening traces, measured with Au, Pt, and Pt-Ir tips, are shown in Figure 2 and 3, respectively. Electrical and thermal conductance are linearly connected, resulting in the presentation of steps and the formation of plateaus as a result of atomic rearrangements and conductance quantization at the same tip-MEMS displacements and demonstrating excellent agreement in accordance with the Wiedemann-Franz Act. The thermal delay noticed in the experiment. The signal is caused by the thermal time constant of the MEMS, which is about 20 milliseconds. We have been able to collect many hundreds of these opening traces, which has allowed us to construct two-dimensional (2D) histograms in order to statistically examine Figures 1 and 2 show the link between thermal and electrical conductivity. 2(a)–2(c). In order to decrease the impacts of low-pass filtering on the thermal signal, we concentrated the study on traces that had electrical plateaus that lasted for at least 10 milliseconds. In reality, fast breaking curves would just muddy the surface. The single atom peak is hidden by the characteristics in the thermal conductance histogram, which makes it difficult to see. Thermal conductance was normalised in this case by the degenerate thermal conductance quantum for the sake of simplicity.



$$G_Q = G_0 L_0 T = 2 \frac{\pi^2 k_B^2 T}{3h}$$

FIG. 3. (a)–(c) Histograms of the plateau duration in the electrical conductance range between 0.8 and 1.3 G_0 for the different tips. (a) 738 traces, (b) 877 traces, and (c) 982 traces. Very short plateaus

in where k_B denotes the Boltzmann constant, h denotes the Planck constant, and T is the average junction temperature. Following the Wiedemann-Franz rule, all of the counts should be accumulated around the same time. The diagonal of the two-dimensional map. The heat transport characteristics of the Au atomic connections are notable in that they are independent of the tip material and are comparable to those of metal contacts in perfect accordance with the Wiedemann-Franz statute, therefore confirming the fact that the contribution of phonons to thermal conductance is insignificant within the realm of experimental ambiguity (10 percent). Furthermore, both the thermal and electrical 1D projections of the 2D histogram demonstrate a rapid increase in temperature. The maximum conductance quantum is located near the middle of the peak. This discovery also shows that the interfacial thermal resistance of the gold layer adhering to the surface of the Pt and Pt-Ir tips is greater than that of the gold layer on the surface of the Pt. Is insignificant in relation to the junction until just a few atom connections are made. Finally, at the actual junction between Au and Pt and Pt-Ir, respectively, Seebeck and

Peltier effects may occur, which must be taken into consideration while conducting experiments. It is possible that systematic mistakes will be introduced into the analysis. We, on the other hand, calculate that the thermoelectric effects generated by the metallic heterojunctions are insignificant under these experimental circumstances ($\Delta T = 14.5 - 40 \text{ K}$) by using the following formula: as well as V_{14} at 40 mV). Furthermore, the observation made by the researchers supports this claim. Peaks in thermal and electrical conductance are seen at the conductance quantum.

Because of a greater possibility of generating single atoms when using platinum and platinum-Ir tips, the increased number of counts at $1 \text{ G}\Omega$ obtained with platinum and platinum-Ir tips may be due to these interactions, or from a longer average plateau lifespan, or both. We created histograms of the length of each event to better comprehend this surprising discovery. $1 \text{ G}\Omega$ plateaus for the distinct tips, which indicate the lifetime distribution of the single Au atom interactions generated on the tips' surfaces. Figure 3: Microelectromechanical systems. Please keep in mind that these histograms were produced from the identical sets of traces as those seen in Fig. We can infer a lot from the graphs. Take note of the fact that the plateau distributions follow the same pattern as the A number of distinct hints point to a similar breaking process. This is especially true in the case of We can rule out the production of single atomic chains at a reasonable pace, because as a result of the absence of peaks at multiples of the Au-Au interatomic spacing, look at the histograms^{33,34}. When the temperature is high, this is to be anticipated. (315 K) and at modest stretching speeds, when the atomic

structure is being broken. The majority of the time, heat activation is used to activate contacts. The most significant distinction is that we detect a for both Pt and Pt-Ir tips. The chance of detecting $1 \text{ G}\Omega$ plateaus lasting longer than 10 ms is around 80% . In the case of Au, the percentage is 50% , but in the case of Au, the percentage is 40% . Additionally, in the case of Pt, a significant component of the traces has an average length of around 50 ms , indicating the creation of a stable junction arrangement over a period of time. The mechanical stability of Au atomic junctions may be affected by a variety of parameters, ranging from the tip shape to the cleanliness of the surface. Understanding the minute intricacies of these systems necessitates the use of microscopes. a continuation of the inquiry that goes beyond the scope of this paper. However, by repeating the tests with various tips and MEMS samples, it is possible to. It was discovered that the results achieved with electrochemically etched Pt were superior. Pt-Ir tips are capable of reproducing the finest results attained with Au tips with relative ease.

This demonstrates that having a mechanically stable tip constructed of a stiff material is beneficial. When it comes to heat transfer measures, metal may be quite advantageous. Being adaptable in terms of the apex material may also be beneficial in this situation. Manufacturing tips with integrated thermocouples^{12,35} and extending their use are both possible. When doing such investigations, Wollaston-like probes are used. As a conclusion, we demonstrated that electrochemically etched Pt and Pt-Ir tips are excellent tools for investigating the heat transport features of Au-Au alloys. Atomic connections are made. Following conventional recipes, they

are reasonably simple to construct, and they may be utilised to generate Au atomic connections on Au surfaces with a high likelihood of forming and mechanical stability. This is incredibly important advantageous for thermal transport studies that need a minimum measurement duration of about one thermal time constant of the system under consideration. The sensor was utilised. We expect that these findings will encourage the combination of STM. Capabilities for imaging combined with heat transport measurements at the atomic scale. A crucial step towards understanding the universe is represented by the atomic scale. Heat transfer systems are controlled and understood using computer simulations. Furthermore, we anticipate that enhanced experimental flexibility will result in improved results. allow for the investigation of the heat conduction characteristics of single moleculesgadgets that are electronic.

REFERENCES

- 1 N. Agrait, A. L. Yeyati, and J. M. Van Ruitenbeek, *Phys. Rep.* 377, 81 (2003).
- 2 F. Schwarz and E. Lortscher, *J. Phys.: Condens. Matter* 26, 474201 (2014).
- 3 A. Jain and A. J. H. Mcgaughey, *Phys. Rev. B* 93, 081206 (2016).
- 4 R. Landauer, *IBM J. Res. Dev.* 1, 223 (1957).
- 5 J. M. Krans, J. M. Van Ruitenbeek, V. V. Fisun, I. K. Yanson, and L. J. De Jongh, *Nature* 375, 767 (1995).
- 6 E. Scheer, N. Agrait, J. C. Cuevas, A. L. Yeyati, B. Ludophk, A. Martin-Rodero, G. R. Bollinger, J. M. van Ruitenbeek, and C. Urbina, *Nature* 394, 154 (1998).
- 7 W. Lee, K. Kim, W. Jeong, L. A. Zotti, F. Pauly, J. C. Cuevas, and P. Reddy, *Nature* 498, 209 (2013).
- 8 M. Tsutsui, T. Kawai, and M. Taniguchi, *Sci. Rep.* 2, 217 (2012).
- 9 C. Evangeli, M. Matt, L. Rincon-Garcia, F. Pauly, P. Nielaba, G. RubioBollinger, J. C. Cuevas, and N. Agrait, *Nano Lett.* 15, 1006 (2015).
- 10 M. Tsutsui, T. Morikawa, A. Arima, and M. Taniguchi, *Sci. Rep.* 3, 3326 (2013).
- 11 N. Mosso, U. Drechsler, F. Menges, P. Nirmalraj, S. Karg, H. Riel, and B. Gotsmann, *Nat. Nanotechnol.* 12, 430 (2017).
- 12 L. Cui, W. Jeong, S. Hur, M. Matt, J. C. Klöckner, F. Pauly, P. Nielaba, J. C. Cuevas, E. Meyhofer, and P. Reddy, *Science* 355, 1192 (2017).
- 13 L. A. Zotti, M. Burkle, F. Pauly, W. Lee, K. Kim, W. Jeong, Y. Asai, P. Reddy, and J. C. Cuevas, *New J. Phys.* 16, 015004 (2014).
- 14 J. C. Klöckner, M. Matt, P. Nielaba, F. Pauly, and J. C. Cuevas, *Phys. Rev. B* 96, 205405 (2017).
- 15 M. Burkle and Y. Asai, *Nano Lett.* 18, 7358 (2018).
- 16 I. H. Musselman, P. A. Peterson, and P. E. Russell, *Precis. Eng.* 12, 3 (1990).
- 17 Y. Nakamura, Y. Mera, and K. Maeda, *Rev. Sci. Instrum.* 70, 3373 (1999).
- 18 L. Olesen, E. Laegsgaard, I. Stensgaard, F. Besenbacher, P. Stoltze, and K. W. Jacobsen, *Phys. Rev. Lett.* 72, 2251 (1994).
- 19 J. I. Pascual, J. Mendez, J. Gomez-Herrero, A. M. Baro, N. Garcia, U. Landman, E. N. B. W. D. Luedtke, and H.-P. Cheng, *J. Vac. Sci. Technol. B* 13, 1280 (1995).
- 20 M. Brandbyge, J. Schiøtz, M. R. Sørensen, P. Stoltze, K. W. Jacobsen, and J. K. Nørskov, *Phys. Rev. B* 52, 8499 (1995).